X-Ray Bursts

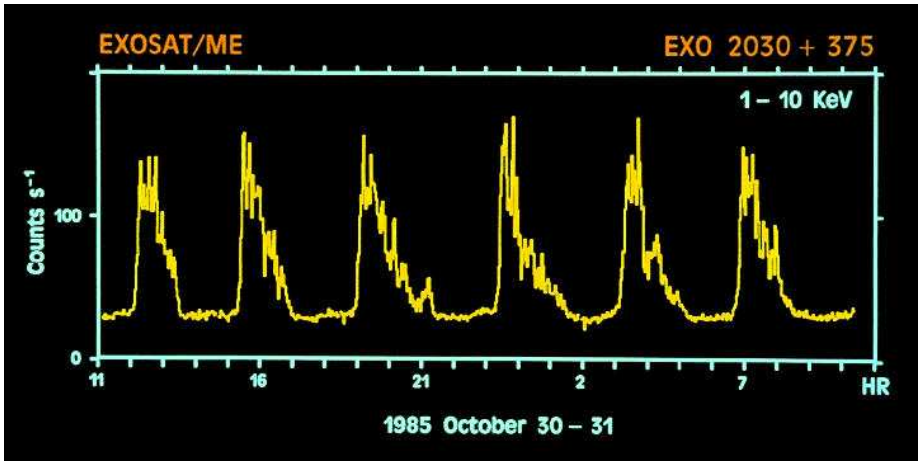

NASA GSFC

X-ray bursts from EXO 2030+375 as seen with EXOSAT.

X-Ray Bursts

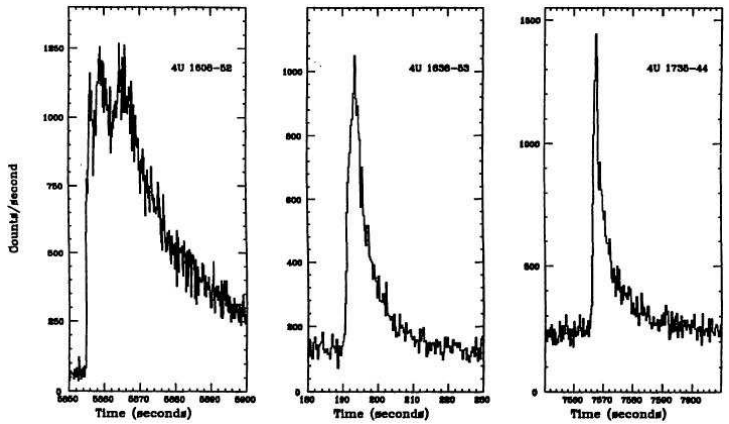

(Lewin, van Paradijs & Taam, 1993, Fig. 3.1)

Bursts come in different shapes, but approximately look like a “FRED”

FRED=Fast Raise and Exponential Decay

X-Ray Bursts

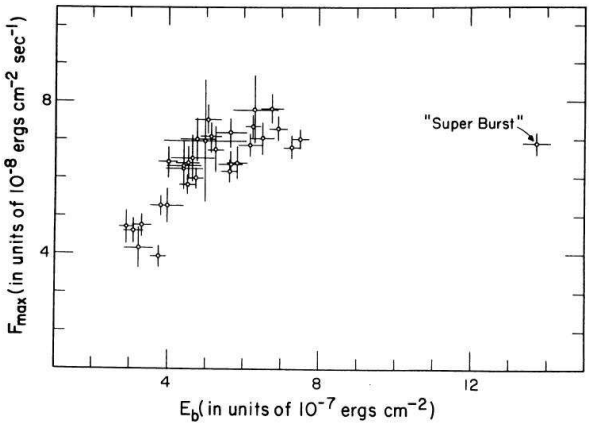

(1728−337; Lewin, van Paradijs & Taam, 1993, Fig. 3.5b)

Peak flux and total fluence of bursts are approxmately linearly correlated

$\Longrightarrow$ more energetic bursts are brighter

X-Ray Bursts

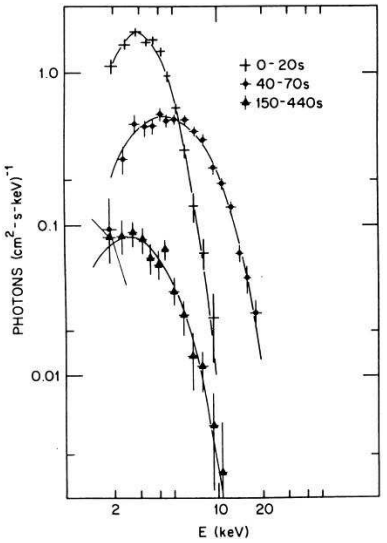

Swank et al. (1977): Spectral shape during the bursts can be well described by a black body spectrum with $kT \sim$ few keV.

$\Longrightarrow$ Optically thick plasma in thermodynamic equilibrium

X-Ray Bursts

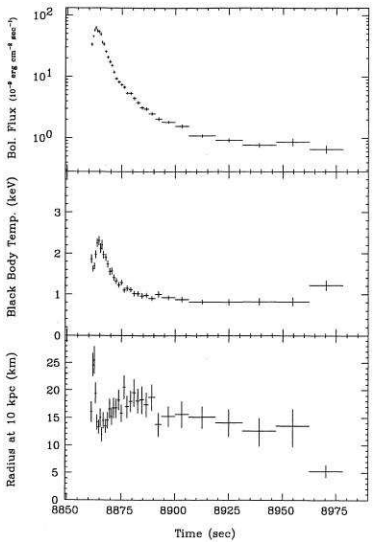

(Lewin, van Paradijs & Taam, 1993, Fig. 3.10)

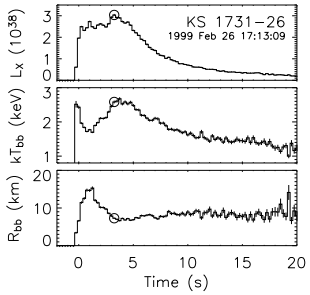

(Galloway et al., 2006, Fig. 1)

Luminosity of a black body: $L_{\rm bb} = R_{\rm bb}^2 \sigma T_{\rm bb}^4$

$\Longrightarrow$ can measure radius of emitter!

$$R = d\sqrt{\frac{4\pi F}{\sigma T^4}}$$

where d estimated distance and F measured flux.

X-Ray Bursts

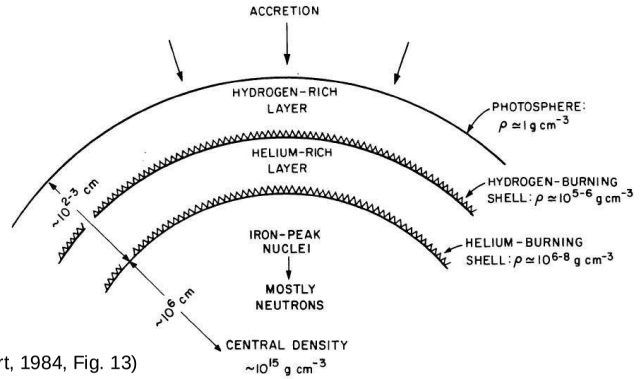

(Joss & Rappaport, 1984, Fig. 13)

Explanation: Bursts are thermonuclear explosions on neutron star surface.

Accretion of hydrogen onto surface

$\Longrightarrow$ H fuses into He (mainly electron captures), nuclear statistical equilibrium below that

$\Longrightarrow$ He shell, and then higher Z.

X-Ray Bursts

Since $T > 10^7$ K: H-burning occurs via the CNO-cycle.

CNO cycle is saturated at $T \gtrsim 8 \times 10^7$ K:

timescale for proton capture $< \beta$-decays of standard CNO-cycle

$t_{1/2} \sim$ 100–1000 s for ^{13}N, ^{14}O, ^{15}O

$\Longrightarrow$ "hot CNO cycle":

$$^{12}\mathrm{C}(p,\gamma)^{13}\mathrm{N}(p,\gamma)^{14}\mathrm{O}(\beta^+)^{14}\mathrm{N}(p,\gamma)^{15}\mathrm{O}(\beta^+)^{15}\mathrm{N}(p,\alpha)^{12}\mathrm{C}$$

This process is instable for

$$\dot{m} < 900\,\mathrm{g\,cm^{-2}\,s^{-1}} \left(\frac{Z_{\rm CNO}}{0.01}\right)^{1/2} \tag{6.36}$$

where Z: mass fraction and where $\dot{m} = \dot{M}/(4\pi R^2)$.

$\Longrightarrow$ Type I burst

X-Ray Bursts

The Energy released during the burst is:

$$E_{\rm burst} = Q\frac{4\pi R^2 H\rho}{m_{\rm H}} \sim 2 - 8 \times 10^{39}\,\mathrm{erg} \tag{6.37}$$

where typical parameters are $R = 10$ km, $H \sim 10^2$ cm, $\rho = 10^6$ g cm^{-3}, and

- H-burning: $Q = 7$ MeV nucleon^{-1}
- He-burning: $Q = 1.5$ MeV nucleon^{-1}

If the whole accreted matter $M_{\rm acc} = 4\pi R^2 H\rho$ is used, then the time averaged burst luminosity is

$$L_{\rm burst} = \frac{E_{\rm burst}}{\Delta t} = Q\frac{\dot{M}}{m_{\rm H}} \tag{6.38}$$

Since the accretion luminosity is

$$L_{\rm acc} = \frac{GM\dot{M}}{R} \tag{6.39}$$

the ratio between persistent and burst emission is

$$\alpha = 30 - 120\left(\frac{M}{M_\odot}\right)\left(\frac{R}{10\,\mathrm{km}}\right)^{-1} \tag{6.40}$$

similar to what is observed.

X-Ray Bursts

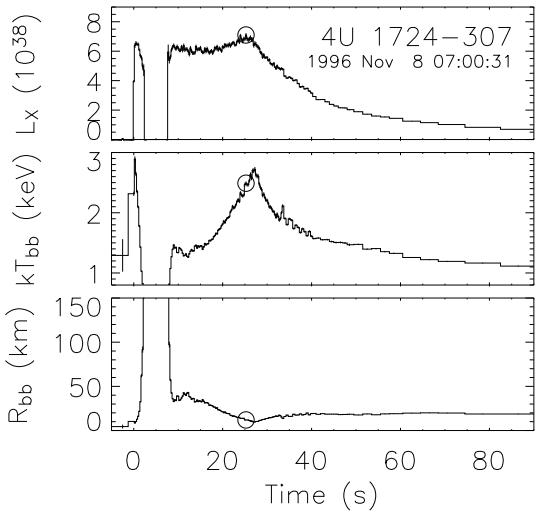

For most luminous bursts (large He fraction):

$L \gtrsim L_{\text{Edd}}$

$\Longrightarrow$ atmosphere "ejected"

$\Longrightarrow$ radius expansion bursts.

Note that outside of bursts $R_{\text{BB}} \sim R_{\text{neutron star}}$!

(Galloway et al., 2006, Fig. 10)

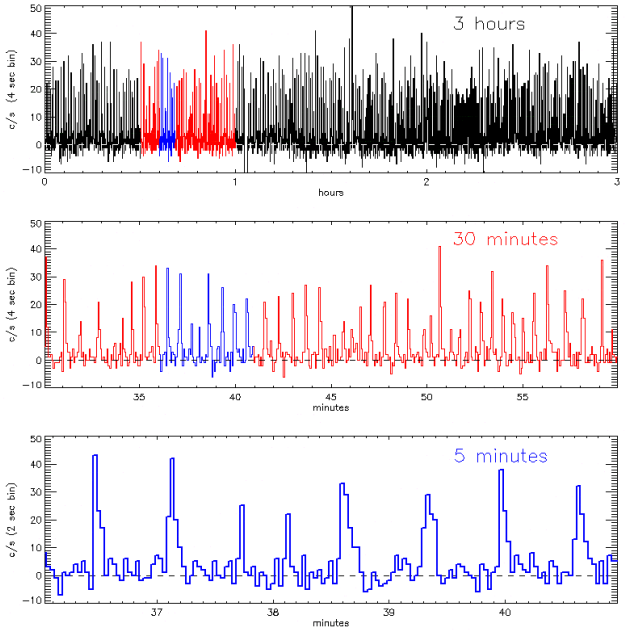

Bursting of the "Rapid Burster" MXB1730−335: Type I and Type II bursts.

Type II bursts: magnetospheric gate model: B-field blocks accretion until $P_{\text{gas}} > P_{\text{mag}} \Longrightarrow$ BOOM.

(Kuulkers et al., 2008)

Neutron Star HMXBs, I

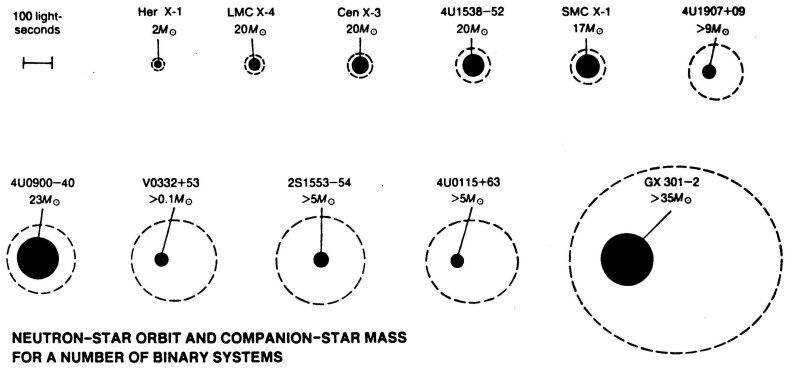

Charles & Seward, 1995, Fig. 7.7a

High-Mass X-ray Binaries: Donor star has early spectral type (O, B), and mass $M \gtrsim 10\, M_\odot$.

Dominant accretion mechanisms: Wind Accretion or Accretion Disk. Optical emission dominated by O or B star.

Neutron Star HMXBs, II

Neutron stars in HMXBs are young neutron stars

$\Longrightarrow$ expected to have strong B-fields!

Neutron stars are formed in supernova explosions.

One of the conserved quantities is the magnetic flux,

$$\Phi = 4\pi R^2 B \quad \Longrightarrow \quad R_{\text{NS}}^2 B_{\text{NS}} = R_*^2 B_* \tag{6.41}$$

or

$$B_{\text{NS}} = B_* \left(\frac{R_*}{R_{\text{NS}}} \right)^2 \tag{6.42}$$

with $R_* \sim 700000$ km, $R_{\text{NS}} = 10$ km and typical pre supernova stellar B-fields of $B_* \sim 100$ G, giving $B_{\text{NS}} = 5 \times 10^9 \times 10^2$ G $= 5 \times 10^{11}$ G.

Young Neutron Stars are expected to have magnetic fields on the order of 10^{12} G (10^8 T).

Theories in which neutron star magnetic fields are formed after the supernova yield similar results.

Neutron Star HMXBs, III

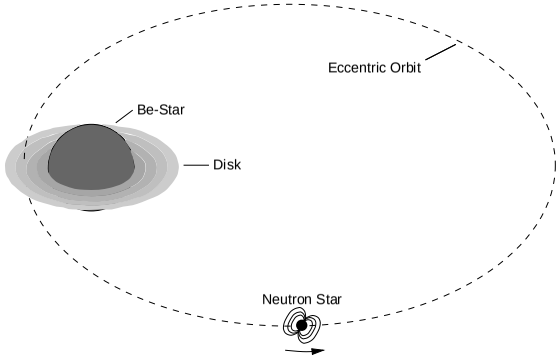

(Kretschmar 1996, Dissertation AIT, Abb. 2.6)

Some early type stars (O9–B2) have very high rotation rates $\Longrightarrow$ Formation of disk-like stellar wind at equator. Line emission from disk: Be phenomenon.

Collision of neutron star with disk results in irregular X-ray outbursts.

Example: A0535+26.

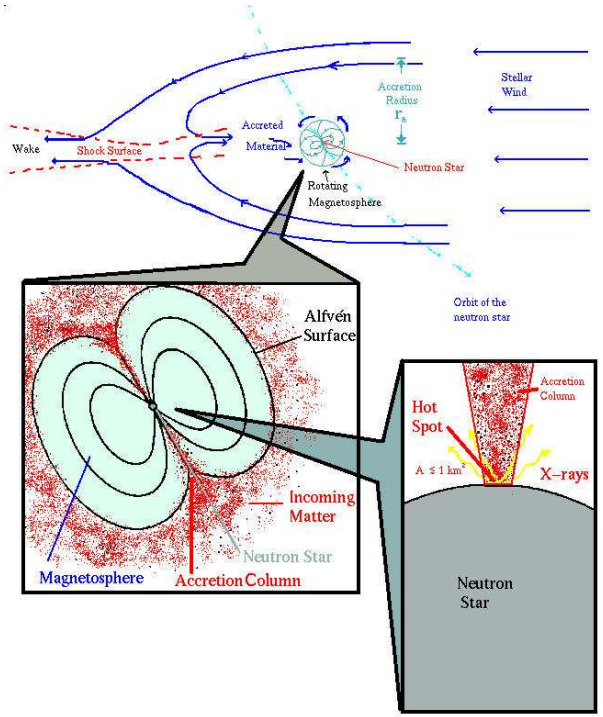

courtesy I. Negueruela, based on Davidson & Ostriker (1973)

Magnetospheric accretion, I

Accretion model has to take into account that central neutron star has $\sim 10^{12}$ G B-field.
Far-field:

$$B(r) = \left(\frac{R}{r}\right)^3 B_\mathrm{p} \quad \text{hence} \quad P_\mathrm{mag} = \frac{B^2}{8\pi} = \left(\frac{R}{r}\right)^6 B_\mathrm{p}^2$$

On the other hand, the accreting material has a ram-pressure

$$P_\mathrm{ram} = \rho v^2 \quad \text{or} \quad P_\mathrm{ram} = \frac{\dot{M}}{4\pi r^2}\left(\frac{2GM}{r}\right)^{1/2}$$

assuming free fall ($v = (2GM/r)^{1/2}$) and spherical symmetry ($\dot{M} = 4\pi r^2 \rho v$).

For $P_\mathrm{mag} > P_\mathrm{ram}$, B-field dominates $\Longrightarrow$ plasma couples to B-field lines at the Alfvén radius

$$r_\mathrm{mag} = \left(\frac{8\pi^2}{G}\right)^{1/7}\left(\frac{R^{12}B_\mathrm{p}^4}{M\dot{M}^2}\right)^{1/7}$$

$$= 1800\,\mathrm{km}\left(\frac{R}{10\,\mathrm{km}}\right)^{12/7}\left(\frac{B}{10^{12}\,\mathrm{G}}\right)^{4/7}\left(\frac{M}{1.4\,M_\odot}\right)^{-1/7}\left(\frac{\dot{M}}{10^{-7}\,M_\odot\,\mathrm{yr}^{-1}}\right)^{-2/7}$$

For typical NS parameters, the accretion close to the NS is dominated by the B-field.

Magnetospheric accretion, III

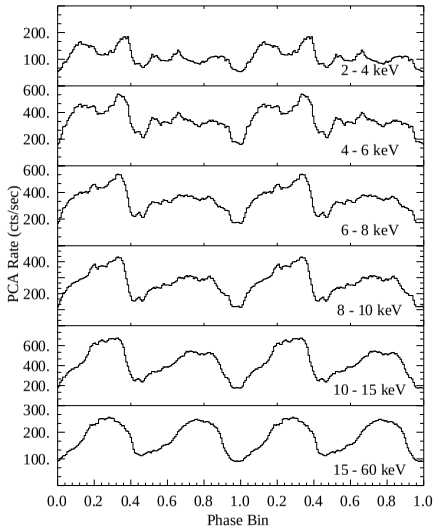

Rotation of accreting neutron star leads to X-ray pulsations.

Typically complex profiles at low E, $\sim$sinusoidal profiles at higher energies $\Longrightarrow$ due to emission characteristics and absorption in accretion flow?

(Kreykenbohm et al., 1999, Vela X-1)

Magnetospheric accretion, IV

At distance r from the Neutron Star, the Keplerian velocity is

$$v = \sqrt{\frac{GM}{r}} \tag{6.43}$$

and therefore the orbital period ("Kepler period") and frequency are

$$P_{\mathrm{K}} = \frac{2\pi r}{v} = \sqrt{\frac{4\pi^2 r^3}{GM}} \iff \Omega_{\mathrm{K}} = \frac{2\pi}{P_{\mathrm{K}}} = \sqrt{\frac{GM}{r^3}} \tag{6.44}$$

For $r = 1800\,\mathrm{km}$ and $M = 1.4\,M_\odot$, $P = 1\,\mathrm{s}$.

Since the magnetic field couples the accretion disk to the neutron star, we expect accreting neutron stars to have periods on the order of one second.

. . . provided the coupling between the accretion disk and the B-field is strong enough

Magnetospheric accretion, V

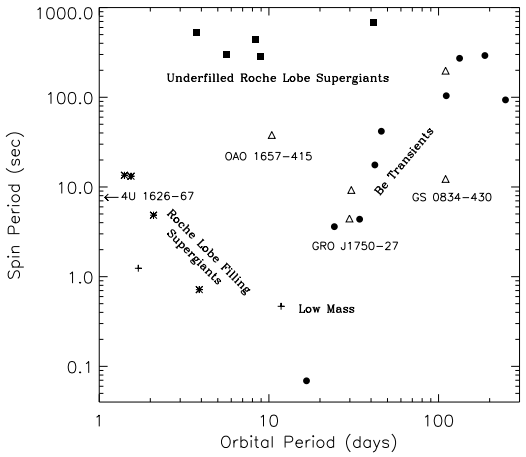

Corbet diagram: Spin period vs. orbital period for HMXB

- Roche lobe overflow: low P_{spin}, low P_{orb}, $L_{\mathrm{X}} \gtrsim 10^{37}\,\mathrm{erg\,s^{-1}}$
- Wind accretors: longer orbital periods (to avoid Roche lobe overflow), $L_{\mathrm{X}} \sim 10^{35-37}\,\mathrm{erg\,s^{-1}}$
- Be systems: correlation between spin and orbital periods (higher P_{orb}: less time to torque neutron star?).

Magnetospheric accretion, VI

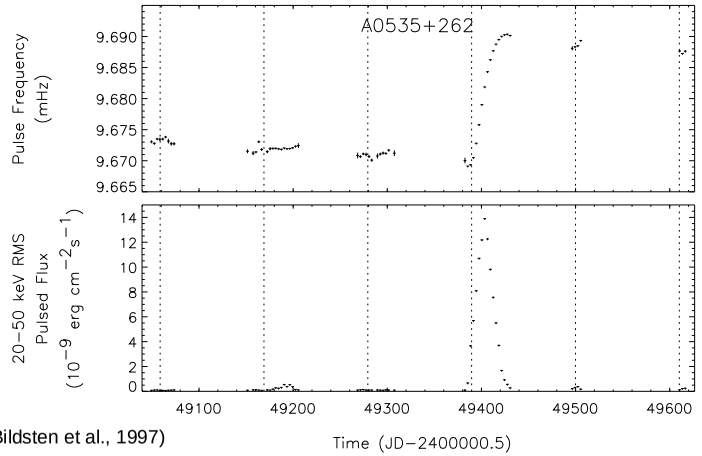

(Bildsten et al., 1997)

Interaction between B-field and accretion disk leads to torques onto neutron stars $\Longrightarrow$ spin up and spin down.

For transient systems such as A0535+26, spin up is correlated with outbursts (i.e., increased $\dot{M}$).

Accretion Column, I

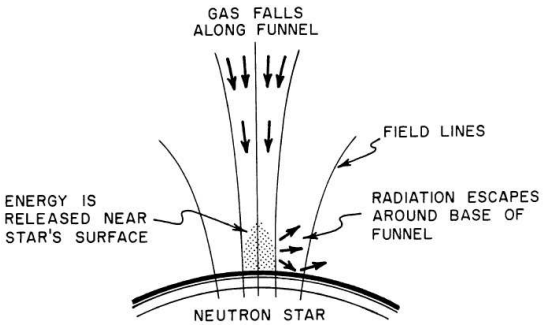

(Ostriker & Davidson, 1973, Fig. 4)

Within R_{mag}, low density material

$\Longrightarrow$ approximate free fall along B-field lines.

Speed at magnetic pole:

$$v = \sqrt{\frac{2GM}{R}} \sim 0.65\,c$$

($\sim$140 MeV nucleon^{-1})

The area of the accreting spot is (for a dipolar B-field):

$$\pi r_0^2 = \pi R^2 \cdot (R/r_{\mathrm{mag}}) \lesssim 1\,\mathrm{km}^2$$

see also Pringle & Rees (1972), Gnedin & Sunyaev (1973), and Inoue (1975).

Accretion Column, II

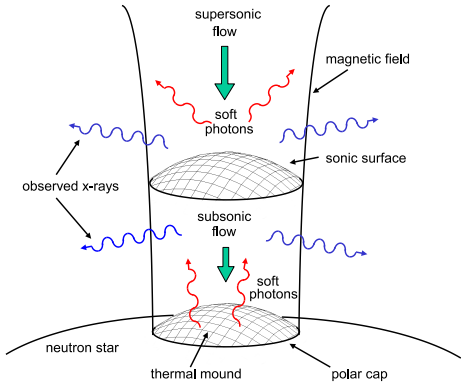

Becker & Wolff (2005a,b, 2007):
Accretion shock dominates formation of observed continuum.

- accretion mound produces soft X-rays (bremsstrahlung)
- X-rays are upscattered in accretion shock (bulk motion Comptonization)
- hard X-rays diffuse through walls of accretion column

Accretion Column, III

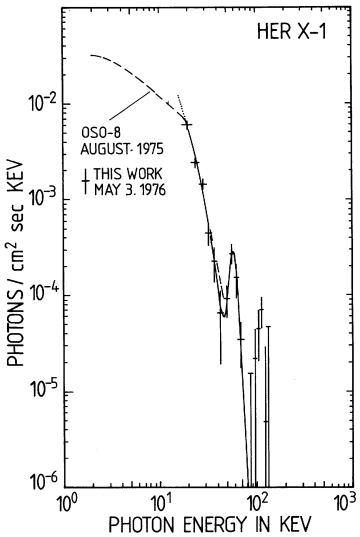

X-ray spectral shape:

- power law continuum with exponential cutoff
  Due to Compton scattering
- normally strong Fe Kα line at 6.4. . . 6.7 keV
  Due to fluorescence in circumstellar material.
- Cyclotron line due to strong B-field

Her X-1 (Trümper et al., 1978)

Accretion Column, IV

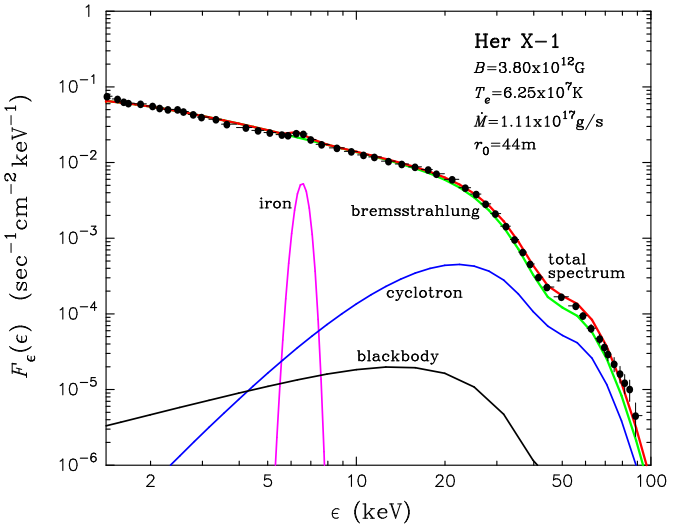

Becker & Wolff (2007, Fig. 6)

Cyclotron Lines, I

Strong field at neutron star's poles introduces exotic physics:
Quantization of electron energies $\perp B$-field lines (Landau levels):

$$E_n = m_e c^2 \frac{\sqrt{1 + 2n(B/B_{\text{crit}}) \sin^2\theta} - 1}{\sin^2\theta} \tag{6.45}$$

$p_\parallel$: momentum of electron $\parallel B$-field, n: major quantum number, B_{crit} is

$$B_{\text{crit}} = \frac{m_e^2 c^3}{e\hbar} \sim 4.4 \times 10^{13}\,\text{G} \tag{6.46}$$

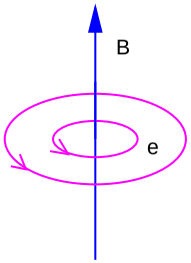

For $B \ll B_{\text{crit}}$, distance between Landau levels:

$$E_{\text{cyc}} = \frac{\hbar e}{m_e c} B = 11.6\,\text{keV}\left(\frac{B}{10^{12}\,\text{G}}\right) \tag{6.47}$$

$(12 - B_{12}$-rule)
$\Longrightarrow$ Cyclotron Resonance Scattering Features ("Cyclotron lines") at

$$E_n = nE_{\text{cyc}} = (1+z)E_{n,\text{obs}} \tag{6.48}$$

$(1 + z \sim 1.25 \ldots 1.4$; grav. redshift!)

In the following, a quick derivation of the basic physics of electrons in strong magnetic fields is given, following Mészáros (1992). Note that this is rather advanced quantum mechanics, and while you should know the end results, the detailed derivation is beyond the scope of the lecture.

The (relativistic) equation of motion of an electron in a magnetic field is given by

$$\frac{d}{dt}(\gamma m \boldsymbol{v}) = \frac{q}{c}\boldsymbol{v} \times \boldsymbol{B} \tag{6.49}$$

where the Lorentz factor, γ, is

$$\gamma = \frac{1}{\sqrt{1-\beta^2}} = \frac{1}{\sqrt{1-\left(\frac{v}{c}\right)^2}} \tag{6.50}$$

If we ignore the radiative losses caused by the acceleration of the electron, then $\gamma =$ const. and the equation of motion is

$$\frac{d\boldsymbol{v}_\parallel}{dt} = 0 \tag{6.51}$$

$$\gamma m \frac{d\boldsymbol{v}_\perp}{dt} = \frac{q}{c}\boldsymbol{v}_\perp \times \boldsymbol{B} \tag{6.52}$$

where $\boldsymbol{v}_\parallel$ and $\boldsymbol{v}_\perp$ are the components of the velocity vector parallel and perpendicular to the magnetic field, respectively.

Since the force on $\boldsymbol{v}_\perp$ is perpendicular to $\boldsymbol{v}_\perp$, the motion of the electron will be described by a circular motion around the $\boldsymbol{B}$-field line together with constant motion parallel to the magnetic field.

It is easy to see (check for yourself!) that the frequency of motion around the magnetic field, the so-called *gyrofrequency* is given by

$$\omega_B = \frac{qB}{\gamma mc} = \frac{\omega_\mathrm{L}}{\gamma} \tag{6.53}$$

where the *Larmor frequency* is given by

$$\omega_\mathrm{L} = \frac{qB}{mc} \tag{6.54}$$

The Larmor frequency is the frequency of a non-relativistically gyrating electron.

Caveat emptor: many authors do not make a distinction between the Larmor frequency and the gyrofrequency. Be careful!

The radius of gyration, the *gyro radius*, is

$$r_g = \gamma v_\perp \frac{mc}{qB} = \gamma r_\mathrm{L} \tag{6.55}$$

and again, many authors do not distinguish between the gyro radius and the *Larmor radius*.

Finally, the cyclotron energy of the electron is

$$\hbar\omega_g = \hbar\frac{qB}{\gamma mc} \tag{6.56}$$

This classical approach performed so far is valid as long as the Larmor radius is large compared to the de Broglie wavelength of the electron,

$$\lambda_\mathrm{e} = \frac{\hbar}{p} = \frac{\hbar}{\gamma m v_\perp} \tag{6.57}$$

Therefore, QM effects are important once

$$\frac{\hbar}{\gamma m v_\perp} \geq \frac{v\gamma mc}{qB} \tag{6.58}$$

that is, for magnetic fields

$$B \geq \frac{m^2c^3\gamma^2}{q\hbar}\left(\frac{v_\perp}{c}\right)^2 = \gamma^2\beta_\perp^2\frac{m^2c^3}{e\hbar} = \gamma^2\beta_\perp^2 B_\mathrm{c} \tag{6.59}$$

here, $B_\mathrm{c} = m^2c^3/(q\hbar) \sim 4.4 \times 10^{13}$ G is the *critical magnetic field*. This name derives from the fact that the nonrelativistic (!!!) cyclotron energy can be written as

$$\hbar\omega_\mathrm{L} = mc^2\frac{B}{B_\mathrm{c}} \tag{6.60}$$

that is, for $B = B_\mathrm{c}$ the nonrelativistic cyclotron energy equals the electron's rest mass. B_c is thus a natural quantum mechanical measure for the strength of magnetic fields.

Example: For $kT = 10$ keV, $\beta^2 = 5.6 \times 10^{-2}$ and $\gamma \sim 1$, such that for $B \sim 10^{12}$ G quantum mechanics cannot be ignored.

Electrodynamics shows that the generalized momentum for the motion of particles in a magnetic field is

$$\boldsymbol{p} = m\boldsymbol{v} - \frac{e}{c}\boldsymbol{A} \tag{6.61}$$

where $\boldsymbol{A} = \nabla \times \boldsymbol{B}$, and (in the *Landau gauge*)

$$\boldsymbol{A} = \frac{1}{2}\boldsymbol{B} \times \boldsymbol{r} = \frac{1}{2}Br\hat{\varphi} \tag{6.62}$$

where $\hat{\varphi}$ is an unit vector along the azimuthal angle coordinate. The classical equation of motion for these particles is

$$\frac{mv^2}{r} = \frac{qv}{c}B \tag{6.63}$$

and the quantization condition is (similarly to the Bohr atom!)

$$\boldsymbol{p} \times \boldsymbol{r} = n\hbar\hat{B} \tag{6.64}$$

where $\hat{B}$ is an unit vector in the direction of the magnetic field.

Inserting the generalized momentum into the quantization condition gives after some algebra

$$mvr - \frac{1}{2}\frac{eB}{c}r^2 = n\hbar \tag{6.65}$$

After dividing by m and noticing that $v = \omega_g r$ one finds

$$\frac{1}{2}\omega_g r^2 = \frac{n\hbar}{m} \tag{6.66}$$

Using Eq. (6.63), the kinetic energy can then be found from

$$E_n = \frac{1}{2}mv^2 = \frac{evB}{2c}r = \frac{1}{2}\frac{eB}{c}\frac{2n\hbar}{m} = n\hbar\omega_g \tag{6.67}$$

Similarly one obtains for the orbital radii

$$r_n = \sqrt{\frac{2n\hbar c}{qB}} = 2.6\text{Å} \cdot \sqrt{\frac{2n}{B_{12}}} \tag{6.68}$$

where $B_{12} = B/10^{12}$ G.

The proper derivation of the Landau levels starts from the Schrödinger equation for the motion of a charged particle in an electromagnetic field. Using again the Landau gauge, the nonrelativistic Hamiltonian is

$$\hat{H} = \frac{1}{2m}\left(\hat{p} - \frac{q}{c}\hat{A}\right)^2 - \frac{q\hbar}{2mc}\hat{\sigma} \cdot \boldsymbol{B} \tag{6.69}$$

where $\hat{\sigma}$ is the Pauli spin operator.

To solve for the wave function ψ, insert the Hamiltonian into the Schrödinger equation

$$\hat{H}\psi = E\psi \tag{6.70}$$

and perform the ansatz

$$\psi = \exp\left(\frac{i}{\hbar}(p_x x + p_z z)\right)\chi(y) \tag{6.71}$$

After some rather tedious algebra one can then show that the resulting differential equation for χ has the solution

$$E_n = \left(n + \frac{1}{2} + \sigma\right)\hbar\omega_\mathrm{L} + \frac{p_z^2}{2m} \tag{6.72}$$

where $\sigma = \pm 1/2$. This is Eq. (6.47). The exact equation, Eq. (6.45) is obtained from solving the Dirac equation in the presence of a magnetic field. This is beyond the scope of this lecture.

Cyclotron Lines, II

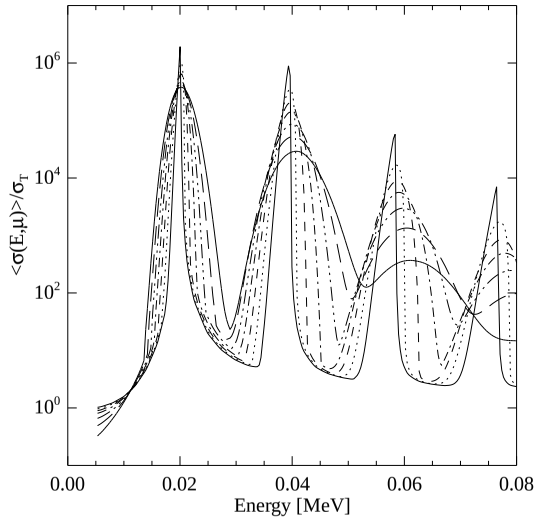

Now look at diagnostics of cyclotron lines in detail

Hot plasma $\Longrightarrow$ thermal broadening:

- Lines narrow perpendicular to B-field
- Lines broad for motion along B-field

Expected line width (Mészáros, 1992)

$$\frac{\Delta E_\mathrm{FWHM}}{E_\mathrm{cyc}} \sim \sqrt{kT_\mathrm{e}}|\cos\theta|$$

(~ 6 keV for $kT_\mathrm{e} = 40$ keV)

$B = 1.7 \times 10^{12}$ G, $kT = E_\mathrm{cyc}/4$, θ: angle between B-field and photon direction; Schönherr et al. (2007), after Araya & Harding (1999)

Cyclotron Lines, III

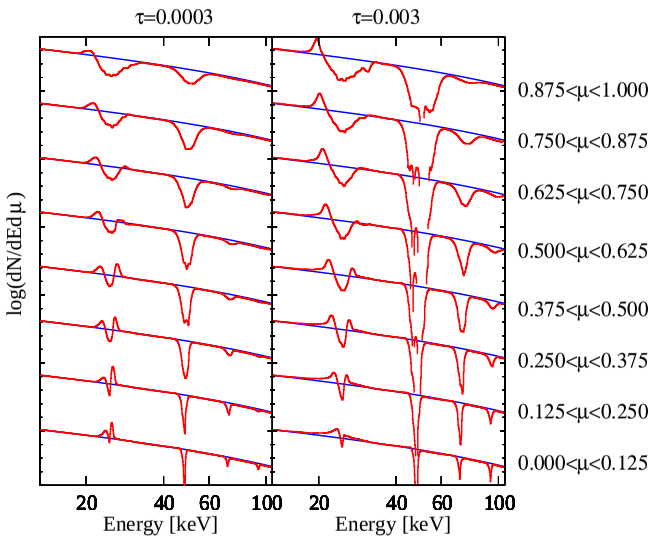

Dependence on optical depth and angle.

Note: resonance optical depth $\sim 10^5 \cdot \tau_T$!

$B = 1.76 \times 10^{12}$ G, $kT_e = 3$ keV; (Schönherr et al., 2007)

Cyclotron Line Sources

Source	E_{cyc} (keV)	P_{puls} (s)	P_{orb} (d)	companion	discovery
4U 0115+63	14, 24, 36, 48, 62	3.6	24.31	Be	HEAO-1 (Wheaton, '79) RXTE, SAX (Heindl '99, Sant.,'99)
4U 1907+09	18, 38	438	8.38	B2 III–IV	SAX (Cusumano, '98)
4U 1538−52	20	530	3.73	B0I	Ginga (Clark, '90)
Vela X-1	24, 52	283	8.96	B0.5Ib	Mir-HEXE (Kendziorra, '92), RXTE (Kreykenbohm, '02)
V 0332+53	27	4.37	34.25	Be	Ginga (Makishima, '90)
Cep X-4	28	66.25	>23	B1	Ginga (Mihara, '91)
Cen X-3	29	4.8	2.09	O6.5II	SAX (Santangelo, '98) RXTE (Heindl, '98)
X Per	29	837	250.3	B0 III–Ve	RXTE (Coburn, '01)
XTE J1946+274	36	15.8	169.2	B0-1V-IVe	RXTE (Heindl, '01)
OAO 1657−415	36?	37.7	10.4	B0-B6Ia-Iab	SAX (Orlandini, '99)
4U 1626−67	37	7.66	0.028	WD?	SAX (Orlandini, '98) RXTE (Heindl, '98)
GX 301−2	37	690	41.5	B1.2Ia	Ginga (Mihara, '95)
Her X-1	41	1.24	1.7	A9-B	Ballon-HEXE (Trümper, '78)
A0535+26	50, 110	105	110.58	Be	HEXE (Kendziorra, '92, '94), CGRO (Maisack, '97)
LMC X-4	100?	13.5	1.41	O7IV	SAX (LaBarbera, '01)

A0535+26, I

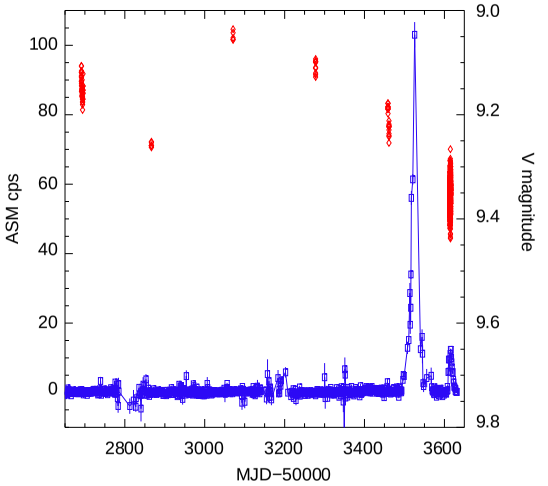

- transient O9.7IIIe/NS binary, 111 d orbit, outbursts in 1975, 1980, 1983, 1989, 1994, 2005
- giant outburst in May/June: over 1 Crab, but: too close to the Sun
- second weaker outburst: ∼300 mCrab in August/September, ToO observations by *INTEGRAL* and *RXTE*

A0535+26, II

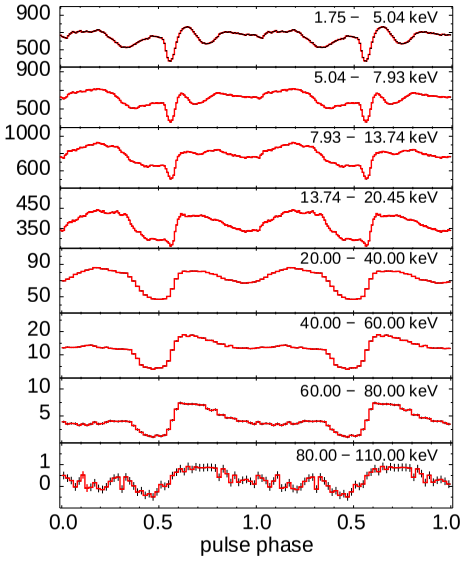

- Pulse period: 103.3920(4) s
- narrow feature at low energies: accretion stream?

(Caballero et al., 2007)

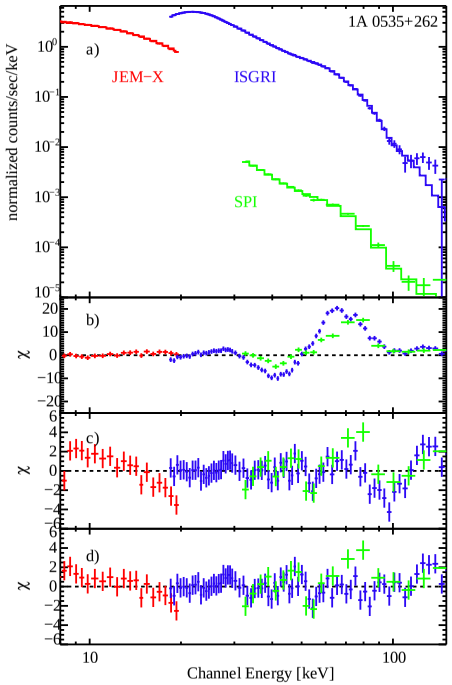

- 2 CRSFs
  - $E_{\mathrm{cyc},1} \sim 45\,\mathrm{keV}$, $\tau_1 \sim 0.5$
  - $E_{\mathrm{cyc},2} \sim 100\,\mathrm{keV}$, $\tau_2 \sim 0.6$
- *RXTE* and *INTEGRAL* consistent!

  and confirming earlier claims for a lower line

(Caballero et al., 2007)

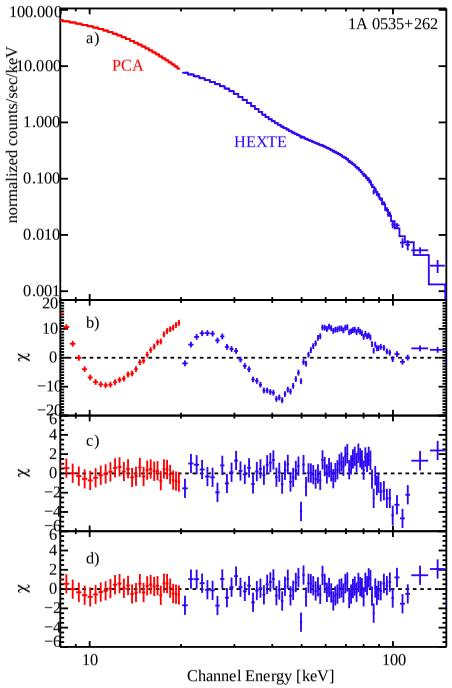

- 2 CRSFs
  - $E_{\mathrm{cyc},1} \sim 45\,\mathrm{keV}$, $\tau_1 \sim 0.5$
  - $E_{\mathrm{cyc},2} \sim 100\,\mathrm{keV}$, $\tau_2 \sim 0.6$
- *RXTE* and *INTEGRAL* consistent!

  and confirming earlier claims for a lower line

(Caballero et al., 2007)

4U1907+09

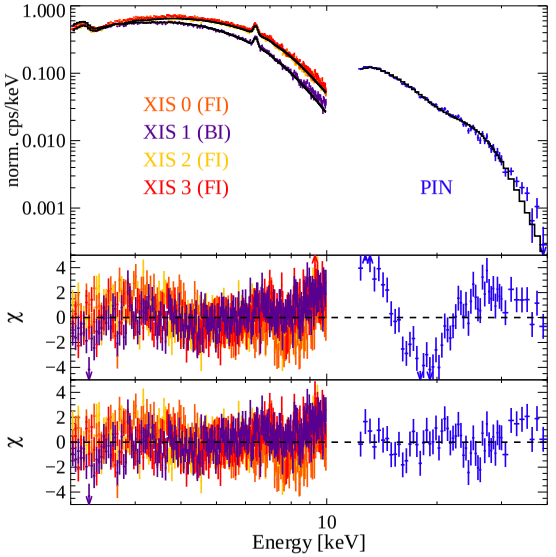

4U1907+09, 2004 December outburst: $E_{\mathrm{cyc}} = 19.7(4)$ keV, $\sigma = 3.3(3)$ keV, in agreement with earlier results (e.g., *INTEGRAL*).

Pottschmidt et al. (2007)

V0332+53

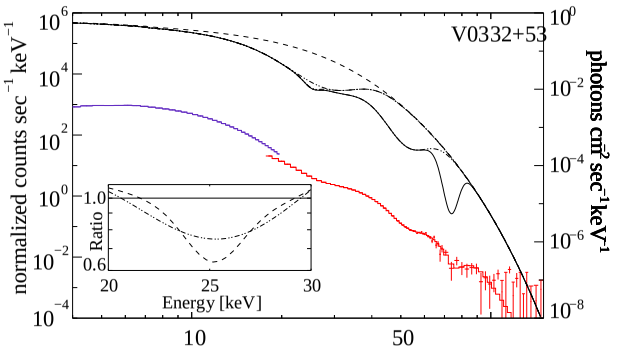

(Pottschmidt et al., 2005)

V0332+53: Cyclotron lines at 27, 51, and 74 keV; complex fundamental.

2nd source after 4U 0115+63 with more than 2 lines.

Line ratios $\neq 2$, agrees with QED prediction; also require scattering angle of $\gtrsim 60°$, in agreement with expectation from resonant cross-section.

Cen X-3

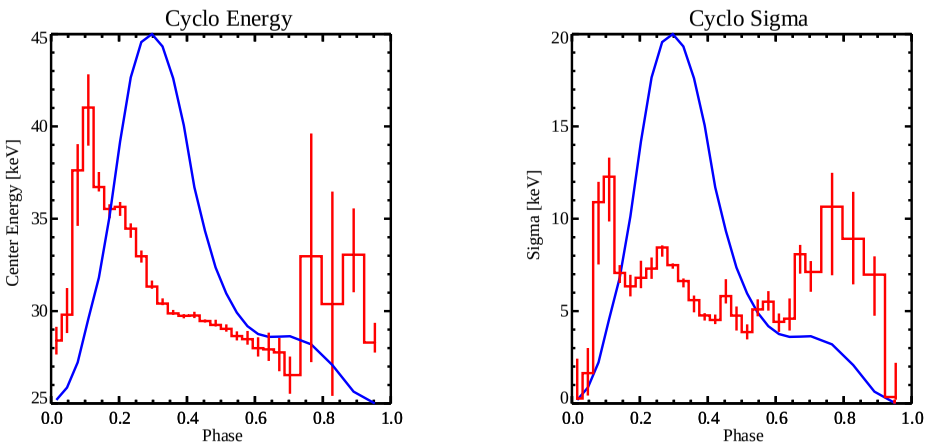

Cen X-3 (Suchy et al., 2008)

Many cyclotron sources show pulse phase dependence of line parameters.

$\Longrightarrow$ effect of viewing angle / height in accretion column?

Luminosity Dependence

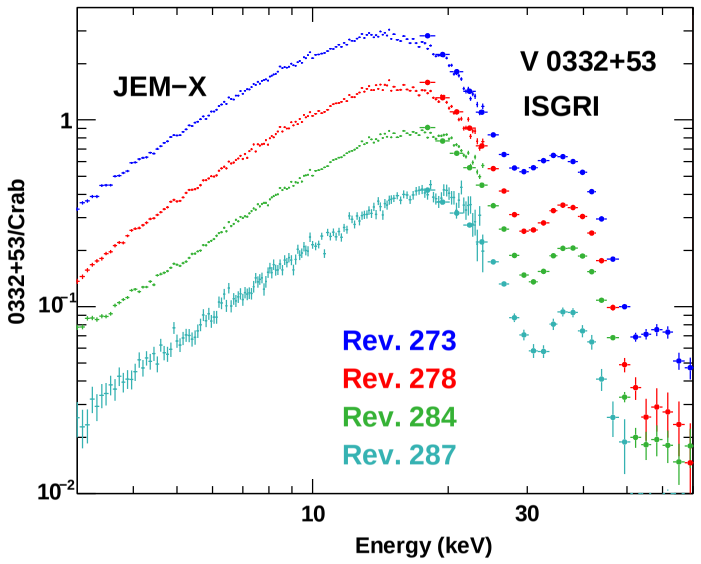

V0332+53: Energy of fundamental cyclotron line changes over outburst

(Mowlavi et al., 2006)

Luminosity Dependence

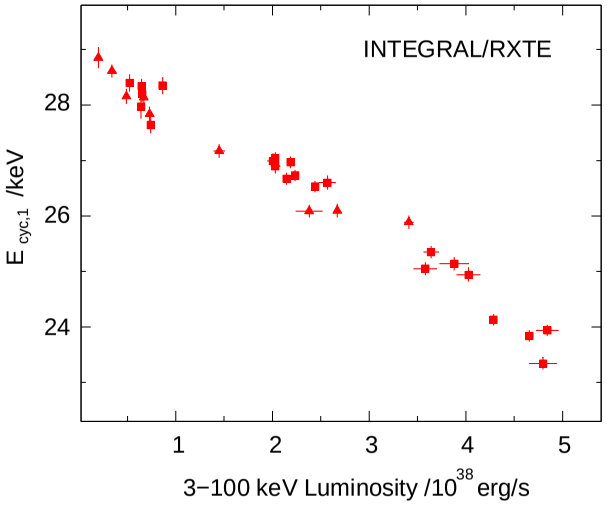

V0332+53: Cyclotron line energy depends on luminosity

$\Longrightarrow$ change of height of accretion column with $\dot{M}$

(Tsygankov et al., 2006)

Luminosity Dependence

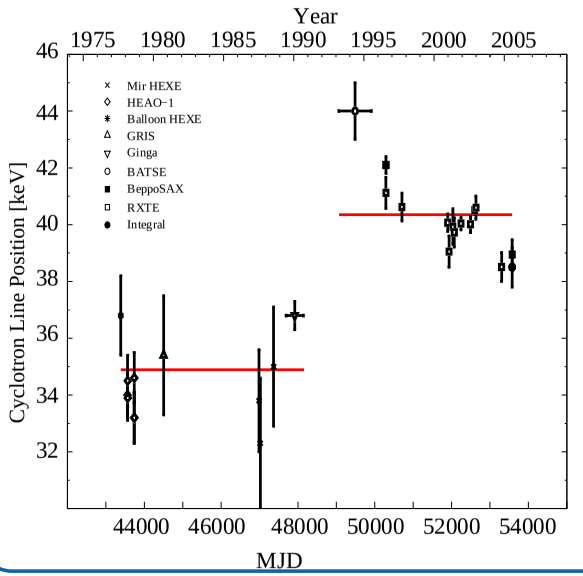

The cyclotron line in Her X-1 shows significant secular variability!

Staubert et al. (2007)